RESEARCH NOTE

CrossMark

Notch signals modulate *lgl* mediated tumorigenesis by the activation of JNK signaling

Maimuna Sali Paul, Ankita Singh, Debdeep Dutta, Mousumi Mutsuddi[*] and Ashim Mukherjee[*]

Abstract

Objectives: Oncogenic potential of Notch signaling and its cooperation with other factors to affect proliferation are widely established. Notch exhibits a cooperative effect with loss of a cell polarity gene, *scribble* to induce neoplastic overgrowth. Oncogenic Ras also show cooperative effect with loss of cell polarity genes such as *scribble* (*scrib*), *lethal giant larvae* (*lgl*) and *discs large* to induce neoplastic overgrowth and invasion. Our study aims at assessing the cooperation of activated Notch with loss of function of *lgl* in tumor overgrowth, and the mode of JNK signaling activation in this context.

Results: In the present study, we use *Drosophila* as an in vivo model to show the synergy between activated Notch (N^{act}) and loss of function of *lgl* (*lgl-IR*) in tumor progression. Coexpression of N^{act} and *lgl-IR* results in massive tumor overgrowth and displays hallmarks of cancer, such as MMP1 upregulation and loss of epithelial integrity. We further show activation of JNK signaling and upregulation of its receptor, Grindelwald in N^{act}/*lgl-IR* tumor. In contrast to previously described $Notch^{act}$/$scrib^{-/-}$ tumor, our experiments in N^{act}/*lgl-IR* tumor showed the presence of dying cells along with tumorous overgrowth.

Keywords: Notch, *lgl*, *Drosophila*, Tumor overgrowth, JNK signaling, Cell death

Introduction

In the past decade, a keen interest has been shown to explore the oncogenic cooperation with loss of cell polarity in tumor progression and malignancy. Studies in *Drosophila* have revealed that the oncogenic form of Ras cooperates with loss of tumor suppressors, namely *scrib*, *lgl* and *dlg* to cause tumor cell invasion [1, 2]. The oncogenic form of Notch has also shown to cooperate with $scrib^{-/-}$ to induce neoplastic overgrowth [2]. The loss-of-function mutation of Scribble complex genes (*scrib*, *lgl* and *dlg*) results in disruption of epithelial integrity followed by neoplastic tissue hyperproliferation [3–5]. However, the tumor formation caused by loss of *scrib, lgl* and *dlg* has been found to be restricted by the compensatory JNK mediated apoptosis [2, 6–8]. Among the Scrib complex genes, *lgl* was the first neoplastic tumor suppressor gene described in *Drosophila* [9]. The phenotypes of *lgl* mutant tissues show close similarity with that of the human epithelial cancers [10–12]. Although it has been shown that Notch cooperates with $scrib^{-/-}$ to induce neoplastic growth, it is still unknown whether Notch works in the same way with loss-of-function of *lgl* also. Recently, Lgl has been shown to regulate Notch signaling via endocytosis [13]. However, it gives no substantial evidence on coupling of *lgl*-Notch effect on tumorigenesis. In the present study, we checked the effect of a tumor suppressor gene mutation, *lgl*, in activated Notch background, and found that *lgl* downregulation synergizes with activated Notch to induce overgrowth and migratory behavior. Here, we show that N^{act}/*lgl-IR* tissues display the hallmarks of tumor overgrowth. Moreover, our study revealed that the effect of N^{act}/*lgl-IR* tumor is mediated by the activation of JNK signaling through the upregulation of its receptor, Grindelwald.

Main text

Methods

Detailed description of methods used in this study is provided in Additional file 1.

*Correspondence: mousumi@bhu.ac.in; mousumi_mutsuddi@yahoo.com; amukherjee@bhu.ac.in; ashim04@gmail.com
Department of Molecular and Human Genetics, Banaras Hindu University, Varanasi 221 005, India

Paul *et al. BMC Res Notes* (2018) 11:247

Page 2 of 9

Fig. 1 Oncogenic Notch synergizes with *lgl-IR* to induce tissue overgrowth. Fluorescent micrographs of eye imaginal discs and larval brains are shown. *ey-GAL4/+* (control) eye imaginal disc shows expression of GFP (**a**) and MMP1 (**a′**). *ey-GAL4* driven *UAS-N^{act}* results in enlarged disc size (**b**) and shows slight enhancement in MMP1 expression (**b′**). *UAS-lgl-IR* eye disc driven by *ey-GAL4* (**c**) induces MMP1 expression (**c′**). *UAS-N^{act}* coexpressed with *UAS-lgl-IR* results in massively overgrown eye discs (**d**) and significant enhancement in MMP1 expression throughout the tissue (**d′**) compared to that of only *lgl-IR* (**c′**) or only *Notch^{act}* (**b′**) overexpressed eye discs. Images **a″–d″** are merges of those in **a–a′**, **b–b′**, **c–c′** and **d–d′** with DAPI, respectively. Expression of GFP and MMP1 in brains of *ey-GAL4* driven *UAS-N^{act}* (**f, f′**) and *UAS-lgl-IR* (**g, g′**) remain similar as of wild-type brain (**e, e′**). **h** *UAS-N^{act}* and *UAS-lgl-IR* coexpressed brain shows massive expression of GFP in the optic lobes and in ventral nerve cord (arrowhead marks the expression of GFP in VNC). **h′** The optic lobes and VNC of *N^{act}/lgl-IR* brain shows extensive expression of MMP1 (arrow marks the expression of MMP1 in VNC). Images **e″–h″** are merges of those in **e–e′**, **f–f′**, **g–g′** and **h–h′** with DAPI, respectively. All eye discs are oriented with dorsal to the left and anterior to the top position. Dorsal view of the brains is shown. Scale bars, 50 μm (**a–d**, **a′–d′**, **a″–d″**) and 100 μm (**e–h**, **e′–h′**, **e″–h″**)

Results

Oncogenic Notch synergizes with RNAi mediated downregulation of *lgl* to promote tissue overgrowth

Coexpression of both *lgl-IR* and *Notch^{act}* in the *Drosophila* eye discs using *ey-GAL4* dramatically induced overgrowth (Fig. 1d, d″) as compared to that of only *N^{act}* overexpressed (Fig. 1b, b″) or only *lgl-IR* overexpressed (Fig. 1c, c″) eye discs. To further describe the phenotype of *N^{act}/lgl-IR* tumor, expression of Matrix metalloproteinase 1 (MMP1) was monitored. MMPs are enzymes with clear association to tumor cell invasion and cancer progression [14, 15]. Coexpression of *Notch^{act}* and *lgl-IR* resulted in massive upregulation of MMP1 expression throughout the entire eye disc (Fig. 1d′) as compared to that of only *N^{act}* or only *lgl-IR* (Fig. 1b′, c′). Further, we extended our observation into the brain since *ey-GAL* is mildly expressed in the brain also. Except endogenous expression, no MMP1 activation was observed in the *ey-GAL4* driven *lgl-IR* (Fig. 1g′) and *N^{act}* larval brain (Fig. 1f′). In case of *Notch^{act}/lgl-IR* larval brain, excessive amount of GFP marked cells with enhanced MMP1 expression was observed in the optic lobes (Fig. 1h, h′). The increment in GFP and MMP1 expression was also found in the ventral nerve cord (VNC) of *Notch^{act}/lgl-IR* larval brain (Fig. 1h, h′ marked with arrows). This indicates that the weak expression of *ey-GAL4* in VNC is also inducing MMP1 expression in *Notch^{act}/lgl-IR* tissue. When we quantified the amount of GFP in upper region of VNC, a significant increment in the amount of GFP in *Notch^{act}/lgl-IR* was found as compared to that of the controls (Additional file 2: Figure S1a). We also quantified the presence of MMP1 in the VNC of *Notch^{act}/lgl-IR* (Additional file 2: Figure S1b), which clearly shows a significant increase as compared to that of the controls. Moreover, transcript levels of *mmp1* in the cephalic complex were also found to be upregulated in *Notch^{act}/lgl-IR* tumor as compared to that of the controls (Additional file 2: Figure S1c).

In order to examine the cytoskeleton network and cell–cell adhesion, we marked the tissues with phalloidin and adherens junction marker proteins, Armadillo (Arm) and Cadherin (*D*E-Cad). The F-actin network marked by phalloidin revealed a defective actin cytoskeleton network in *N^{act}/lgl-IR* tumor tissues compared to that of controls (Additional file 3: Figure S2). In the same way, the localization of *D*E-Cad and Arm were also deregulated in *N^{act}/lgl-IR* tumorous eye discs (Additional file 4: Figure S3a–d, e–h). We, next, determined if neuronal differentiation was defective in *N^{act}/lgl-IR* tumor using a neuronal marker, Elav that marks the differentiated neurons in eye disc and brain. Remarkably, coexpression of *N^{act}* and *lgl-IR* led to severe loss of Elav positive cells in the eye disc and abnormal expression of Elav in the optic lobes indicating an impaired neuronal differentiation (Additional file 4: Figure S3i–l, m–p).

In parallel, we also used dominant-negative version of Notch to see the effect of depletion of Notch signaling on *lgl-IR* tumors. Previously, expression of *mam^{DN}* in *lgl$^-$* tissues partially rescued the *lgl$^-$* mosaic adult eye phenotype [13]. Our analysis also found that reduction of Notch signaling partially rescued the phenotypes of *lgl* loss-of-function flies (Additional file 5: Figure S4). Thus, our analysis support the notion that the *lgl* loss-of-function wing phenotype is dependent on elevated Notch signaling, consistent with the previous study [13].

Involvement of JNK pathway in *N^{act}/lgl-IR* tumor

Previous studies in *Drosophila* have revealed that oncogenic Ras along with loss of *lgl* or *scrib* or *dlg* induces JNK signaling, which is crucial for tumor invasion [7, 16]. This prompted us to check the expression of Puckered (puc), a transcriptional target of JNK signaling and widely used to check the activation of JNK signaling. An enhancer trap allele, *puc-LacZ* [17] was used to monitor the activation of JNK signaling. Coexpression of both *N^{act}* and *lgl-IR* resulted in intense upregulation of *puc* throughout the wing disc (Fig. 2d), indicating the activation of JNK signaling in *N^{act}/lgl-IR* tumor. We also observed a significant

Paul *et al. BMC Res Notes* (2018) 11:247

Page 3 of 9
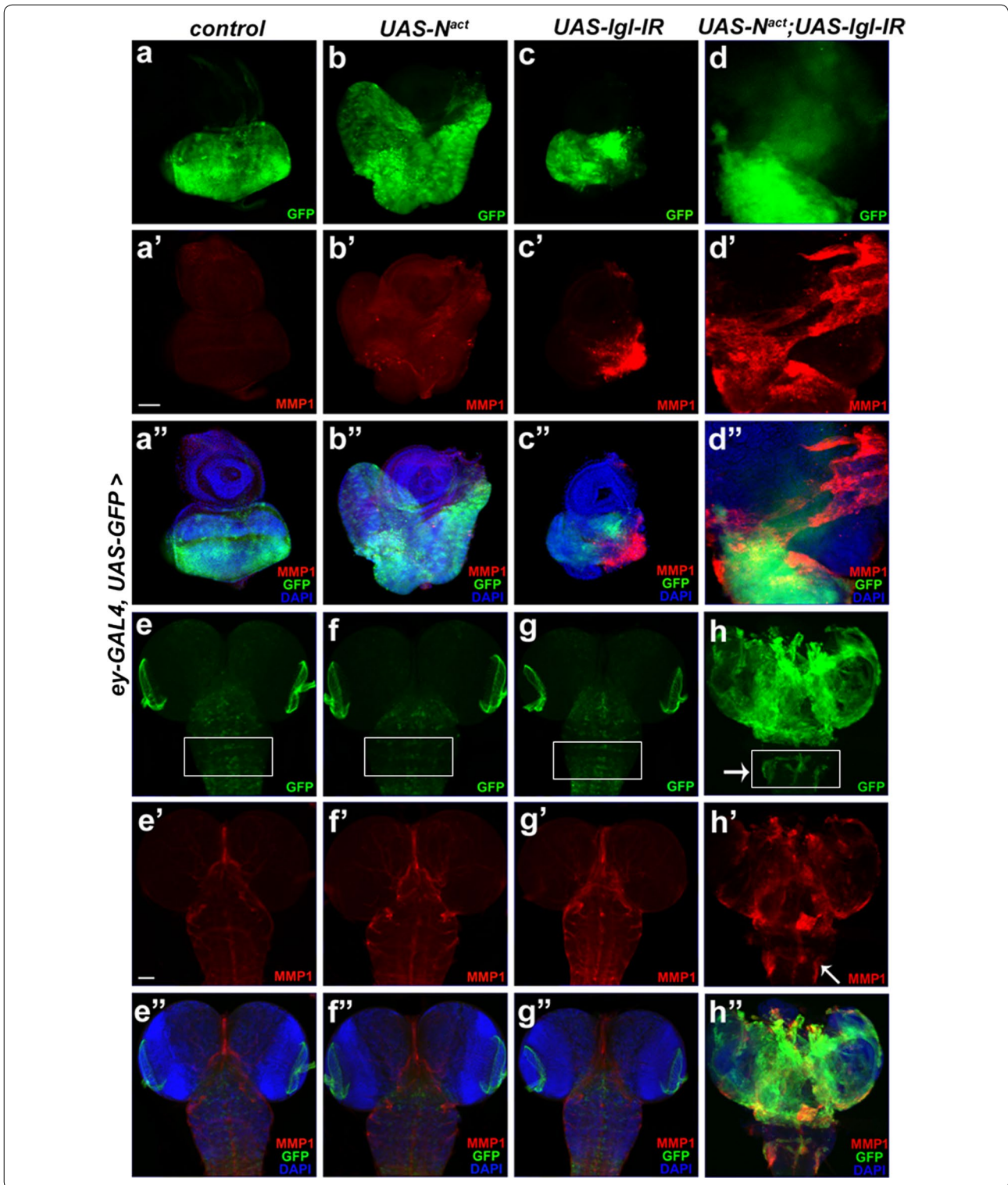
increase in size of the wing disc in N^{act} and *lgl-IR* coexpressed condition compared to that of the wild-type, only N^{act}, and only *lgl-IR* wing discs (Fig. 2i).

To check the mode of activation of JNK signaling, we examined the transcript level expression of ligand *eiger* (*egr*), and its receptor *wengen (wgn),* in N^{act}/*lgl-IR* tumor.

Paul *et al. BMC Res Notes* (2018) 11:247

Page 4 of 9

egr and *wgn* transcript levels were found to be depleted in case of N^{act}/*lgl-IR* tumor as compared to that of the controls (Fig. 2j). Recently, another member in tumor necrosis factor receptor superfamily, Grindelwald (Grnd), found to be associated with loss of cell polarity and neoplastic growth [18]. Interestingly, a significant upregulation of *grnd* transcripts in N^{act}/*lgl-IR* tumor was found, when compared to that of the wild-type, only N^{act} and only *lgl-IR* tissues (Fig. 2j). We went on to check the protein level expression of Egr in N^{act}/*lgl-IR* tumors. Immunostaining with anti-Egr antibody [19] revealed that there is no change in the level of Egr protein expression in *Nact*/*lgl-IR* tumor (Fig. 2h) as compared to that of the wild-type, only N^{act} and only *lgl-IR* tissues (Fig. 2e–g). As Egr is known to be also expressed by the tumor-associated hemocytes, leading to signaling activation [20], these immune cells may be in this case responsible for Grnd activation, but their poor adhesion to the tumor tissue may make them escape Immunofluorescence detection.

To further confirm the involvement of JNK signaling as a downstream event of N^{act}/*lgl-IR* cooperation, we blocked JNK signaling in N^{act}/*lgl-IR* tumor, and checked whether blocking JNK could affect the N^{act}/*lgl-IR* tumor. The massive upregulation of MMP1 in N^{act}/*lgl-IR* tumor (Additional file 6: Figure S5a) was drastically suppressed, when *bsk-DN* (a dominant negative allele of *Drosophila* JNK gene, *basket*) was expressed in the background (Additional file 6: Figure S5b). In addition, coexpression of *bsk-DN* with N^{act}; *lgl-IR* resulted in a reduced wing disc size as compared to N^{act}/*lgl-IR* overexpressed wing disc (Additional file 6: Figure S5c). These results indicate that JNK signaling may be involved in the tumorous overgrowth of N^{act}/*lgl-IR* tissues.
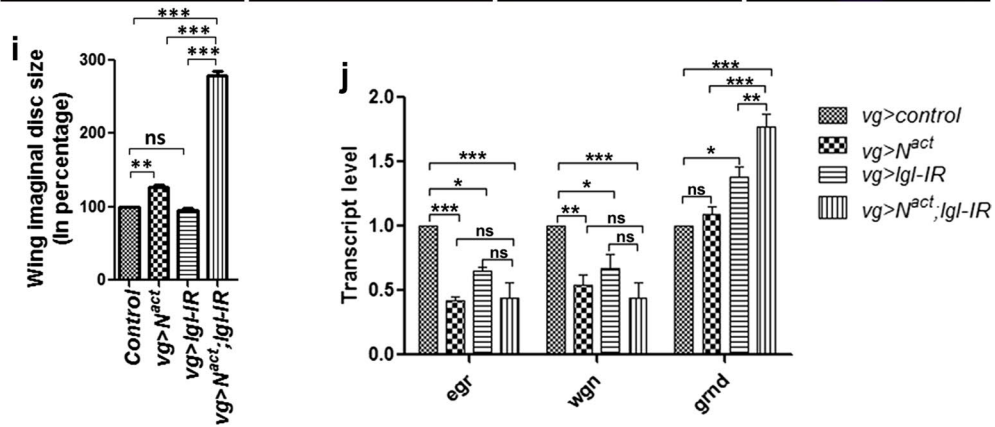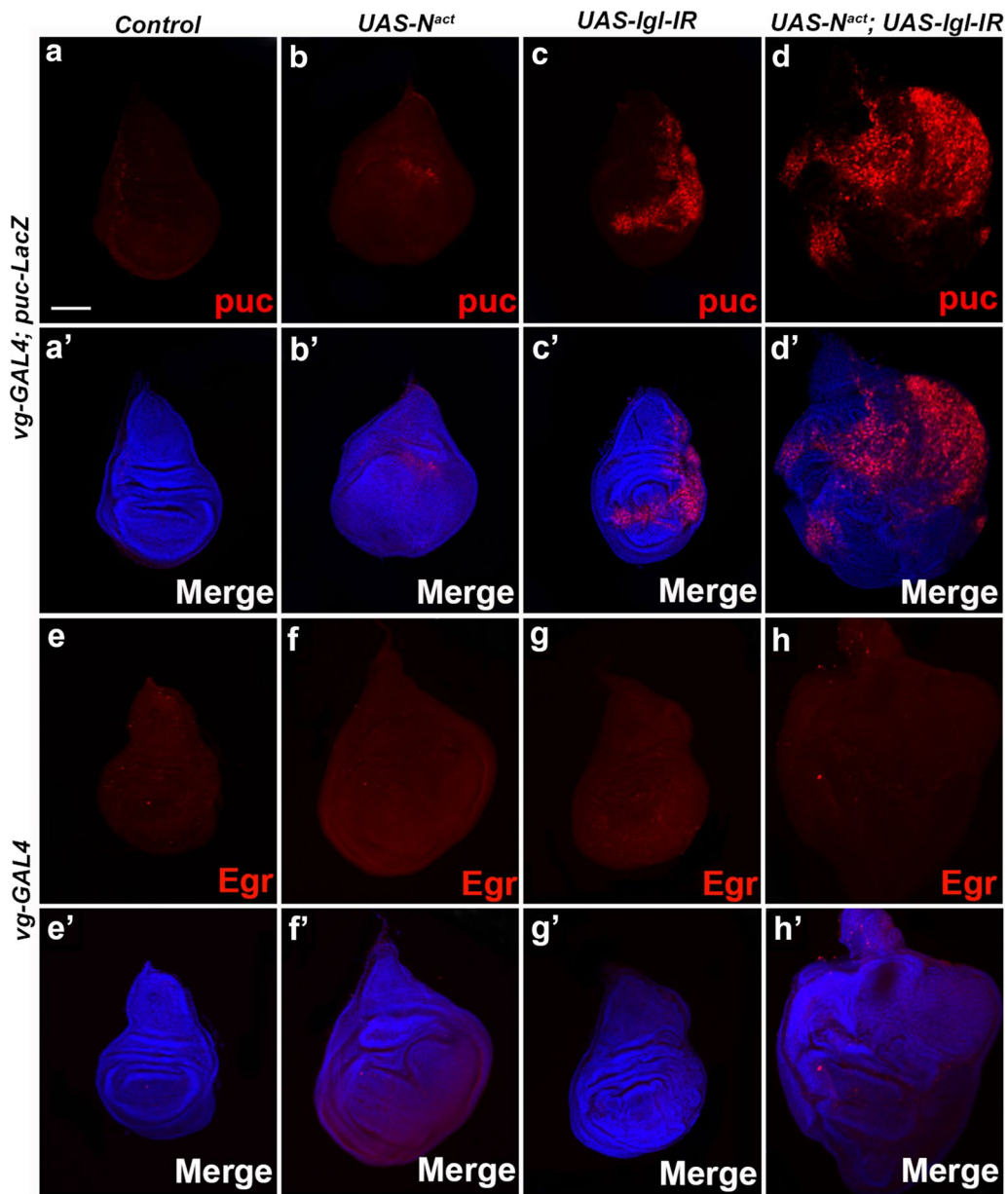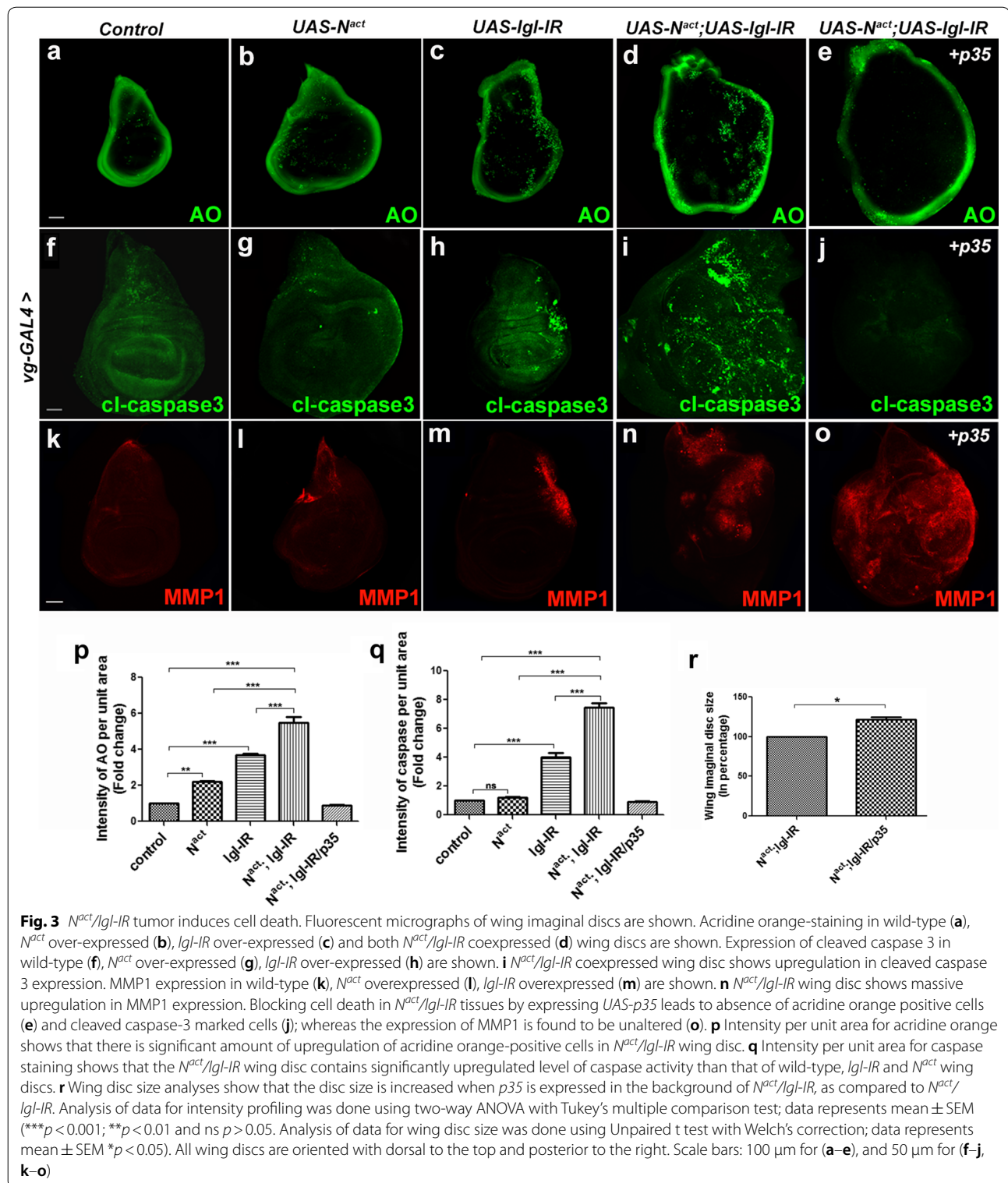
N^{act}/*lgl-IR* tumor induces cell death
Eluding apoptosis is considered as one of the acquired capabilities of many types of cancer; however, studies also explain that elevated oncogenic signaling induces apoptosis or senescence [21]. When we checked the status of cell death in N^{act}/*lgl-IR* tumor, we observed a significant amount of acridine orange (Compare Fig. 3d with a–c) and caspase positive cells (Compare Fig. 3i with f–h) indicating severe cell death. Since loss of *lgl* in a tissue known to induce cell competition to remove the unfit cells [22], dying cells in N^{act}/*lgl-IR* tissue could be an indication of cell competition. To check the effect of cell death on overgrowth and MMP1 expression, we blocked cell death by expressing a caspase inhibitor, p35 (Fig. 3e, j). It was found that blocking cell death in N^{act}/*lgl-IR* overexpressed condition did not obstruct MMP1 expression (Fig. 3o). Coexpression of *p35* with N^{act}/*lgl-IR* resulted in an increased wing disc size as compared to N^{act}/*lgl-IR* overexpressed wing disc (Fig. 3r). As the caspase inhibitor, p35 is known to block cell death [23], the increase in the tissue size is expected since blocking cell death in N^{act}/*lgl-IR* tumor allowed more cells to overgrow that, in turn, increased the disc size.

Discussion
In the present study, we unveil a cooperation of Notch with RNAi-mediated downregulation of a polarity cum tumor suppressor gene, *lgl* to promote tumor overgrowth. Our data, presented here, illustrate that coexpression of N^{act} and *lgl-IR* in *Drosophila* eye disc results in overgrowth, loss of positional clues and upregulation of MMP1 expression, which is less prevalent in only N^{act} overexpression or only *lgl-IR* overexpression. Earlier the loss of polarity gene *scribble* found to cooperate with Notch signaling to promote neoplastic overgrowth [2]. Another two independent studies of similar context show that oncogenic Ras cooperates with loss of cell polarity genes (*lgl, scrib, dlg*) to induce metastasis and secondary tumor formation at distant sites [7, 14]. Interestingly, we found that Notch synergizes with loss of *lgl* to promote tumorous overgrowth and elevated expression of MMP1, and inhibiting Notch signaling rescues the defects caused by loss of *lgl*. It indicates the potential function of Notch signaling

Paul *et al. BMC Res Notes* (2018) 11:247

Page 5 of 9

Paul *et al. BMC Res Notes* (2018) 11:247

Page 6 of 9

Fig. 3 N^{act}/*lgl-IR* tumor induces cell death. Fluorescent micrographs of wing imaginal discs are shown. Acridine orange-staining in wild-type (**a**), N^{act} over-expressed (**b**), *lgl-IR* over-expressed (**c**) and both N^{act}/*lgl-IR* coexpressed (**d**) wing discs are shown. Expression of cleaved caspase 3 in wild-type (**f**), N^{act} over-expressed (**g**), *lgl-IR* over-expressed (**h**) are shown. **i** N^{act}/*lgl-IR* coexpressed wing disc shows upregulation in cleaved caspase 3 expression. MMP1 expression in wild-type (**k**), N^{act} overexpressed (**l**), *lgl-IR* overexpressed (**m**) are shown. **n** N^{act}/*lgl-IR* wing disc shows massive upregulation in MMP1 expression. Blocking cell death in N^{act}/*lgl-IR* tissues by expressing *UAS-p35* leads to absence of acridine orange positive cells (**e**) and cleaved caspase-3 marked cells (**j**); whereas the expression of MMP1 is found to be unaltered (**o**). **p** Intensity per unit area for acridine orange shows that there is significant amount of upregulation of acridine orange-positive cells in N^{act}/*lgl-IR* wing disc. **q** Intensity per unit area for caspase staining shows that the N^{act}/*lgl-IR* wing disc contains significantly upregulated level of caspase activity than that of wild-type, *lgl-IR* and N^{act} wing discs. **r** Wing disc size analyses show that the disc size is increased when *p35* is expressed in the background of N^{act}/*lgl-IR,* as compared to N^{act}/*lgl-IR*. Analysis of data for intensity profiling was done using two-way ANOVA with Tukey's multiple comparison test; data represents mean±SEM (***$p < 0.001$; **$p < 0.01$ and ns $p > 0.05$. Analysis of data for wing disc size was done using Unpaired t test with Welch's correction; data represents mean±SEM *$p < 0.05$). All wing discs are oriented with dorsal to the top and posterior to the right. Scale bars: 100 μm for (**a**–**e**), and 50 μm for (**f**–**j**, **k**–**o**)

during *lgl* mediated tumor development. Our data also show distorted epithelial integrity in N^{act}/*lgl-IR* tumor that point towards epithelial to mesenchymal transition, where tightly joined epithelial cells with regularly spaced cell–cell junctions convert to mesenchymal cells which are of irregular shape without tight intracellular adhesion [24].

Paul *et al. BMC Res Notes* (2018) 11:247

Page 7 of 9

Further, we found upregulation of JNK signaling and its receptor Grindelwald in N^{act}/lgl-IR tumor. Two previous studies have shown that Notch cooperates with two different proteins to induce proliferation and metastasis by the activation of JNK signaling in ligand-dependent and -independent manner [25, 26]. In case of N^{act}/lgl-IR tumor, we show that the transcript levels of *egr* (ligand) and *wgn* (receptor) were not upregulated, whereas a significant upregulation of *grnd* transcripts in the N^{act}/lgl-IR tumor was observed. Earlier the active form of Grnd has shown to activate JNK signaling in vivo [18]. Thus, in case of N^{act}/lgl-IR tumor, JNK signaling might get activated through Grindelwald. Previously, it has been shown that JNK signaling can initiate tumor initiation and growth in Eiger-independent manner also [27].

Another most important hallmark of almost all types of cancer is the ability to evade apoptosis that, in turn, helps tumor cell population to increase in number [21]. In other similar tumor models such as $Ras^{v12}/dlg^{-/-}$, dying cells of $dlg^{-/-}$ clones evade apoptosis in presence of oncogenic Ras, where JNK signaling switches its role from proapoptotic to progrowth [7]. In contrast, $Ras/scrib^{-/-}$ and $Ras/lgl^{-/-}$ tumors were reported to show apoptosis [22, 28]. However, $Notch/scrib^{-/-}$ tumor did not show the presence of apoptosis [29]. In our case, N^{act}/lgl-IR tumor resulted in severe apoptosis along with strong overgrowth and MMP1 expression. These dying cells in N^{act}/lgl-IR tumor might be the indication of cell competition as there is a strong proliferation and overgrowth. In case of $N^{act}/scrib^{-/-}$ tumor, Notch is giving growth advantage to $scrib^{-/-}$ tissues by preventing cell death. However, in case of N^{act}/lgl-IR wing discs, activation of Notch failed to restrict the cell death caused by loss of *lgl*; rather its activation induces further cell death. These differences indicate that although oncogenic cooperation with loss of cell polarity results in similar tumor cell migration but certain property like cell death occurs depending on the context.

Limitations

- The present study is not the first one to show the cooperation between Notch and loss of cell polarity genes. Activated Notch is known to cooperate with another cell polarity gene, *scribble*, to induce neoplastic overgrowth.
- In the present study, experiments were performed using RNAi line of *lgl*, but not with the *lgl* loss-of-function mutants.

Additional files

Additional file 1. Materials and methods.

Additional file 2: Figure S1. Quantification of GFP and MMP1 in the VNC of N^{act}/lgl-IR tumor (**a**) GFP quantification in VNC shows a four-fold increment in the amount of GFP positive cells in N^{act}/lgl-IR as compared to that of the wild-type, only N^{act} and *lgl-IR* overexpressed tissues. **b** MMP1 quantification in VNC shows around four-fold increase in N^{act}/lgl-IR, whereas only N^{act} and *lgl-IR* overexpressed tissues show almost same level of MMP1 in VNC as of wild-type. **c** Real-Time PCR analysis shows significant increase in *mmp1* transcripts in the cephalic complex of N^{act}/lgl-IR as compared to that of wild-type, only N^{act} or only *lgl-IR* tissues. Data was normalized to *rps17*. Analysis of data was done using One-way ANOVA with Tukey's multiple comparison test; data represents mean ± SEM (***$p < 0.001$ and ns $p > 0.05$).

Additional file 3: Figure S2. N^{act}/lgl-IR tumor leads to distorted actin cytoskeleton. Coexpression of N^{act} and *lgl-IR* causes distorted actin cytoskeleton organization (**d**) compared to that of wild-type (**a**), only N^{act} overexpressed (**b**) and only *lgl-IR* overexpressed condition (**c**). F-actin was marked using phalloidin. Scale bars: 10 μm (a-d).

Additional file 4: Figure S3. N^{act}/lgl-IR shows hallmarks of migratory tumor. Fluorescent micrographs of eye imaginal discs and larval brains are shown. **a**, **a′** Endogenous Cadherin and (**e**, **e′**) Armadillo localize at the adherens junctions and marks the photoreceptors in the *ey-GAL4*/+ eye imaginal discs. Morphogenetic furrow in **a** and **e** is marked with an arrow. Overexpression of N^{act} leads to overgrown discs and the localization pattern of Cadherin (**b**, **b′**) and Armadillo (**f**, **f′**) have been modified. Overexpression of *lgl-IR* results in distorted localization of Cadherin (**c**, **c′**) and Armadillo (**g**, **g′**). Coexpression of N^{act} and *lgl-IR* in eye imaginal disc causes complete deformation of Cadherin (**d**, **d′**) and Armadillo (**h**, **h′**) localization pattern. Images **a′–d′**, **e′–h′** are higher magnification of the square region from **a–d**, **e–h**. **i** Expression of Elav, a marker for differentiated neurons in wild-type eye discs is shown. **j** Overexpression of N^{act} in eye disc shows increased expression of Elav, probably due to overproliferation of the disc. **k** *lgl-IR* over-expressed eye disc shows comparatively less Elav-positive cells. **l** Interestingly, N^{act} and *lgl-IR* coexpressed eye disc shows hardly any Elav-positive cells. Images **i′**, **j′**, **k′** and **l′** are merges of GFP along with **i**, **j**, **k** and **l**, respectively. Elav expression in the brains of N^{act} (**n**) and *lgl-IR* (**o**) driven by *ey-GAL4* is found to be similar to that of the wild-type brain (**m**). **p** Coexpression of N^{act} and *lgl-IR* resulted in an abnormal expression pattern of Elav, where clump like distribution is found in the optic lobes (marked with arrow). Images **m′**, **n′**, **o′** and **p′** are merges of GFP along with **m**, **n**, **o** and **p**, respectively. Scale bars: 50 μm (**a–d**, **e–h**, **i–l**, **i′–l′**), 5 μm (**a′–d′**, **e′–h′**) and 100 μm (**m–p**, **m′–p′**). All eye discs are oriented with dorsal to the left and anterior to the top. Ventral view of the brains is shown.

Additional file 5: Figure S4. Lowering the dose of Notch partially rescues *lgl-IR*-induced MMP1 expression and restores the adult wing. **a** MMP1 expression in wild-type wing disc is shown. **b** Overexpression of only *Notch-DN* did not induce expression of MMP1. **c** Overexpression of *lgl-IR* induces MMP1 expression in the wing disc. **d** Coexpression of *Notch-DN* in *lgl-IR* background partially rescues the expression of MMP1 caused by *lgl-IR* overexpression. **a′**, **b′**, **c′** and **d′** are merges of DAPI along with **a**, **b**, **c** and **d**, respectively. Moreover, Coexpression of *Notch-DN* with *lgl-IR* resulted in reduced wing disc size as compared to that of only overexpression of *lgl-IR* (**i**). **e** GFP marked vestigial domain in wing disc is shown. **e′** is the merge image of DAPI along with (**e**). **f** Overexpression of *Notch-DN* resulted in held out wings with wing nicking phenotype. **g** Overexpression of *lgl-IR* using *vg-GAL4* led to necrotic lesions followed by deformation of adult wings. **h** Coexpression of *Notch-DN* with *lgl-IR* partially restored deformed adult wings. **j** Phenotype penetrance in adult flies is shown for each genotype; the phenotype observed in *Notch-DN* show 100% penetrance and around 70% *lgl-IR* flies showed deformed wings. In case of *Notch-DN; lgl-IR* flies, around 60% flies showed the depicted phenotype and, the rest of the flies showed less developed wings but

Paul *et al. BMC Res Notes* (2018) 11:247

Page 8 of 9

they were not of the *lgl-IR* category. Analysis of data was done using One-way ANOVA with Tukey's multiple comparison test; data represents mean ± SEM (***$p < 0.001$ and ns $p > 0.05$). All wing discs are oriented with dorsal to the top and posterior to the right. Scale bar: 50 μm (**a**–**d**, **a′**–**d′**).

Additional file 6: Figure S5. Inhibition of JNK pathway suppresses the N^{act}/lgl-IR tumor growth and MMP1 expression. Fluorescent micrographs of wing imaginal discs are shown. **a** Overexpression of both N^{act} and *lgl-IR* in wing imaginal disc using *vg-GAL4* resulted in massive upregulation of MMP1. **b** Coexpression of bsk^{DN} in the background of N^{act} and *lgl-IR* resulted in the suppression of MMP1 expression. **a″**–**b″** is the merge images of **a**–**a′** and **b**–**b′**. **c** The N^{act}/lgl-IR wing disc size was significantly reduced, when *bskDN* was expressed in the background. Analysis of data was done using Unpaired t test with Welch's correction; data represents mean ± SEM **$p < 0.01$. All wing discs are oriented with dorsal to the top and posterior to the left. Scale bar: 50 μm (a–a″, b–b″).

Abbreviations

scrib: scribble; lgl: lethal giant larvae; dlg: discs large; N^{act}: activated Notch; lgl-IR: lgl-RNAi; MMP1: matrix metalloproteinase; VNC: ventran nerve cord; ey-GAL4: eyeless GAL4; Arm: armadillo; *DE*-Cad: *Drosophila* E-Cadherin; Notch-DN: Notch dominant negative; puc: puckered; egr: eiger; wgn: wengen; grnd: grindelwald; bsk-DN: basket-dominant negative.

Authors' contributions

AM and MSP involved in conception and design of the study. MSP performed the experiments, analyzed the data and drafted the manuscript. DD involved in critically revising the original draft. AS and MM were involved in analysis and interpretation of the data. All authors read and approved the final manuscript.

Competing interests

The authors declare that they have no competing interests.

Availability of data and materials

Data available on request from the corresponding author.

Consent for publication

Not applicable.

Ethics approval and consent to participate

Not applicable.

Publisher's Note

Springer Nature remains neutral with regard to jurisdictional claims in published maps and institutional affiliations.

References

1. Pagliarini AR, Xu T. A genetic screen in *Drosophila* for metastatic behavior. Science. 2003;302:1227–31.
2. Brumby AM, Richardson HE. scribble mutants cooperate with oncogenic Ras or Notch to cause neoplastic overgrowth in *Drosophila*. EMBO J. 2003;22:5769–79.
3. Gateff E, Schneiderman HA. Developmental studies of a new mutant of *Drosophila melanogaster*: lethal malignant brain tumor (l(2)gl 4). Am Zool. 1967;7:760.
4. Stewart M, Murphy C, Fristrom JW. The recovery and preliminary characterization of X chromosome mutants affecting imaginal discs of *Drosophila melanogaster*. Dev Bio. 1972;1927:71–83.
5. Bilder D, Perrimon N. Localization of apical epithelial determinants by the basolateral PDZ protein Scribble. Nature. 2000;403:676–80.
6. Uhlirova M, Jasper H, Bohmann D. Non-cell-autonomous induction of tissue overgrowth by JNK/Ras cooperation in a *Drosophila* tumor model. Proc Natl Acad Sci USA. 2005;102:13123–8.
7. Igaki T, Pagliarini RA, Xu T. Loss of cell polarity drives tumor growth and invasion through JNK activation in *Drosophila*. Curr Biol. 2006;16:1139–46.
8. Froldi F, Ziosi M, Garoia F, Pession A, Grzeschik AN, Bellosta P, et al. The*lethal giant larvae* tumour suppressor mutation requires dMyc oncoprotein to promote clonal malignancy. BMC Biol. 2010;8:1–16.
9. Gateff E. The genetics and epigenetics of neoplasms in *Drosophila*. Biol Rev. 1978;53:123–68.
10. Froldi F, Ziosi M, Tomba G, Parisi F, Garoia F, Pession A, et al. Drosophila lethal giant larvae neoplastic mutant as a genetic tool for cancer modeling. Curr Genom. 2008;9:147–54.
11. Grifoni D, Sollazzo M, Fontana E, Froldi F, Pession A. Multiple strategies of oxygen supplies in *Drosophila* malignancies identify trichogenesis as a novel cancer hallmark. Sci Rep. 2015;5:9061.
12. Calleja M, Morata G, Casanova J. Tumorogenic properties of *Drosophila* epithelial cells mutant for *lethal giant larvae*. Dev Dyn. 2016;245:834–43.
13. Parsons LM, Portela M, Grzeschik NA, Richardson HE. Lgl regulates Notch signaling via endocytosis, independently of the apical aPKC-Par6-Baz polarity complex. Curr Biol. 2014;24:2073–84.
14. Uhlirova M, Bohmann D. JNK and Fos-regulated Mmp1 expression cooperates with Ras to induce invasive tumors in *Drosophila*. EMBO J. 2006;25:5294–304.
15. McCawley LJ, Matrisian LM. Matrix metalloproteinases: multifunctional contributors to tumor progression. Mol Med Today. 2000;6:149–56.
16. Leong GR, Goulding KR, Amin N, Richardson HE, Brumby AE. *scribble* mutants promote aPKC and JNK-dependent neoplasia independently of Crumbs. BMC Biol. 2009. https://doi.org/10.1186/1741-7007-7-62.
17. Shklover J, Mishnaevski K, Levy-Adam F, Kurant E. JNK pathway activation is able to synchronize neuronal death and glial phagocytosis in *Drosophila*. Cell Death Dis. 2015;6:e1649.
18. Andersen SD, Colombani J, Palmerini V, Chakrabandhu K, Boone E, Rothlisberger M, et al. The *Drosophila* TNF receptor Grindelwald couples loss of cell polarity and neoplastic overgrowth. Nature. 2015;522:482–6.
19. Moreno E, Yan M, Basler K. Evolution of TNF signaling mechanisms: JNK dependent apoptosis triggered by Eiger, the *Drosophila* homologue of the TNF superfamily. Curr Biol. 2002;12:1263–8.
20. Cordero BJ, Macagno PJ, Stefanatos KR, Strathdee EK, Cagan LR, Vidal M. Oncogenic Ras diverts a host TNF tumor suppressor activity into tumor promoter. Dev Cell. 2010;8:999–1011.
21. Hanahan D, Weinberg RA. Hallmarks of cancer: the next generation. Cell. 2011;144:646–74.
22. Menéndez J, Pérez-Garijo A, Calleja M, Morata G. A tumor-suppressing mechanism in *Drosophila* involving cell competition and the Hippo pathway. Proc Natl Acad Sci USA. 2010;107:14651–6.
23. Meier P, Silke J, Leevers SJ, Evan GI. The *Drosophila* caspase DRONC is regulated by DIAP1. EMBO J. 2000;19:598–611.
24. Lee MJ, Dedhar S, Kalluri R, Thompson WE. The epithelial–mesenchymal transition: new insights in signaling, development, and disease. J Cell Biol. 2006;172:973–81.
25. Pallavi SK, Ho MD, Hicks C, Miele L, Artavanis-Tsakonas S. Notch and Mef2 synergize to promote proliferation and metastasis through JNK signal activation in *Drosophila*. EMBO J. 2012;31:2895–907.
26. Ho MD, Pallavi SK, Artavanis-Tsakonas S. The Notch-mediated hyperplasia circuitry in *Drosophila* reveals a Src-JNK signaling axis. eLife. 2015;4:e05996.

Paul *et al. BMC Res Notes* (2018) 11:247

Page 9 of 9

27. Muzzopappa M, Murcia L, Milan M. Feedback amplification loop drives malignant growth in epithelial tissues. Proc Natl Acad Sci USA. 2017;114:E7291–300.
28. Kulshammer E, Uhlirova M. The actin cross-linker filamin/cheerio mediates tumor malignancy downstream of JNK signaling. J Cell Sci. 2013;126:927–38.
29. Doggett K, Turkel N, Willoughby LF, Ellul J, Murray MJ, Richardson HE, et al. BTB-zinc finger oncogenes are required for Ras and Notch-driven tumorigenesis in *Drosophila*. PLoS ONE. 2015;10:e0132987.